Accurate Calculations of Ligand Binding Free Energies: Chiral Separation with Enantioselective Receptors

Joseph M. Hayes,* Matthias Stein, and Jörg Weiser

Anterio Consult & Research GmbH, Augustaanlage 26, 68165 Mannheim, Germany

Received: November 6, 2003; In Final Form: January 30, 2004

Qualitatively accurate calculations of ligand binding free energies (BFEs) as applied to chiral selective receptors using the MINTA (mode integration) algorithm are presented. Extensive conformational searches are first performed using a mixed mode Monte Carlo algorithm (MCMM/LMCS) followed by computation of the BFEs using the MINTA approach. The Merck (MMFFs) force field is used throughout. Deficiencies in the default MMFFs partial charges and torsion parameters assigned to atoms directly involved in substrate binding are systematically removed by reparametrization of these parameters using the program PAROPT and on the basis of Jaguar quantum mechanics calculations. The new force field parameters lead to a systematic improvement in qualitative trends of BFE differences ($\Delta\Delta G_{L-D}$) for different receptors as compared with the experimental enantioselectivities (ee's). The results suggest that this method can be extended to a larger and more complex class of receptors such as proteins.

I. Introduction

The preparation of enantiopure compounds for the pharmaceutical and chemical industries is one of the major tasks facing chemists today. Demand for chiral raw materials, intermediates, and active ingredients is predicted to grow by 9.4% annually between 2000 and 2005.[1] While asymmetric synthesis can yield the desired enantiomer almost exclusively on a smaller scale, large-scale industrial production favors liquid-phase separation techniques for both economical and efficiency reasons. These techniques depend on the design of effective enantioselective "synthetic receptors" that bind enantiomers and draw them across phase boundaries. Very often, the separation of enantiomers is not rationalized. Computational chemistry can be a useful tool to support the development of new, cheap, and efficient synthetic receptors. An ideal approach is a computational technique which can directly relate the computed binding free energy (BFE) differences between L and D bound conformations ($\Delta\Delta G_{L-D}$) to the experimental enantioselectivities measured as enantiomeric excess (ee's). This in place, new host compounds can be predicted. However, the estimation of binding affinities for receptor−enantiomer complexes is a major obstacle to rational design of chiral selective receptors.

Accurate computation of binding affinities/binding free energies has received much attention for the most part of the past 30 years. A large range of methods have been proposed. Examples range from fast empirical scoring function methods,[2−7] free energy perturbation (FEP) theory and thermodynamic integration (TI) methods,[8−12] to linear response methods (LRM)[13−18] which lie between the scoring function and FEP/TI approaches in both speed and accuracy. However, still not one method is completely satisfactory. The most elaborate and accurate of the approaches are the FEP and TI methods which are based on statistical perturbation theory. FEP is theoretically rigorous for the calculation of BFEs, explicitly accounting for all enthalpic and entropic contributions in the limit of complete sampling in either molecular (MD) or stochastic (SD) dynamics, Monte Carlo (MC) or MC/SD simulations.[12] FEP has a number of drawbacks. The long simulation runs required generally make FEP impractical for large-scale protein−ligand simulations. Further, the success of FEP simulations is subject to its limitations with respect to adequate sampling.[19−21] The sampling of the conformational space represents a problem when there are significant barriers for conformational interconversion or when conformational space is large and sparsely populated.[19−23] Nevertheless, MD and MC have both been successfully applied to a number of protein−ligand systems.[12,24,25] Jorgensen et al. have shown that Metropolis Monte Carlo (MMC) can be used equally effectively as MD for proteins.[26] Also, while the hybrid simulation technique termed MC/SD can effectively address the sampling problem for certain multiconformational molecules,[27,28] slow convergence on sparsely populated surfaces due to the random nature of the search procedures can be effectively treated using a "smart" Monte Carlo technique such as jumping between wells (JBW).[29,30] Here, results from a previous conformational search are used to direct the simulations toward the low-energy regions of the PES. JBW can be used alone but is also integrated into the MC/SD mixed algorithm (MC(JBW)/SD).[29]

LRM methods were derived as an alternative more rapid approach to FEP, retaining some of the theoretical aspects and features of the FEP methodology.[13−18] The general approach in LRM methods is the same: binding free energies are calculated on the basis of interaction of the ligand with the solvent in the bound complex compared to the interactions (ligand−solvent) of the ligand in solution alone. LRM methods are "semi-empirical", including empirical parameters derived from experimental binding data.[31,32] Jorgensen has found that a more general empirical equation given as a linear combination of scaled physiochemical descriptors is more suitable in some cases.[17,18]

Recently, direct methods have emerged which involve directly computing the configuration integral as the sum of the contributions of low-energy conformational states. Whereas the "mining minima" method evaluates the configuration integral over torsion angles,[33] MINTA (mode integration approach) calculates it over all degrees of freedom for more accurate free energies.[34] MINTA uses an effective Hessian **H**i to integrate in normal mode space

* Corresponding author: Fax +49-(0)621-4004140; Tel +49-(0)621-4004157; e-mail jhayes@anterio.com.

10.1021/jp0373797 CCC: $27.50
Published on Web 03/19/2004

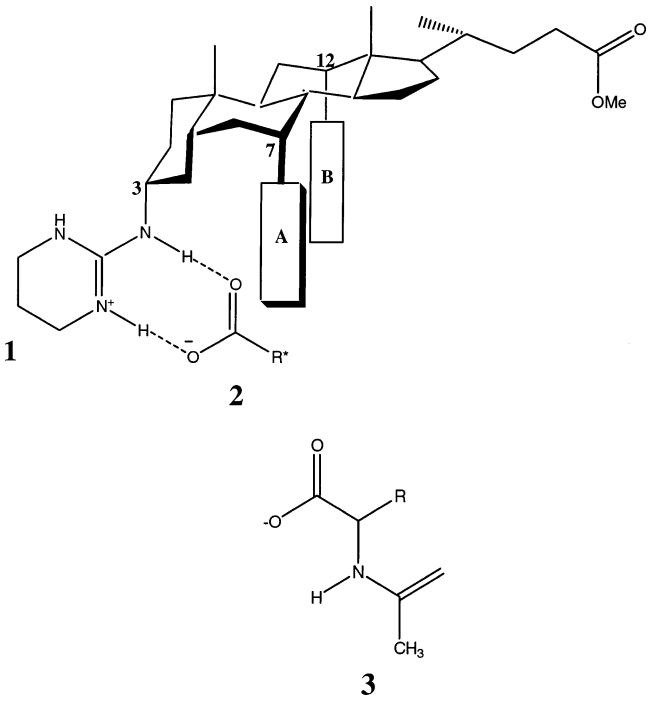

Figure 1. Scaffold for the receptors (**1**) studied in this work which is based on the cholic acid structural backbone. By varying the subunits A and B, different enantioselectivities can be obtained for the bound substrate **2**. An *N*-acyl-α-amino acid (**3**) with R as an isopropyl group (*N*-Ac-DL-valinate) was used as the substrate throughout this study.

for each single conformer. This technique has already been successfully applied to a number of problems: prediction of the enantioselective binding of α-amino acid derivatives to podand ionophore receptors and of peptide ligands to C3-symmetric receptors;[35] calculation of the anomeric free energy of carbohydrates including tetrahydropyran derivatives and pyranose monosaccharides.[34] MINTA's accuracy relies on the results of an exhaustive conformational search of the lowest energy conformers as input but is also heavily dependent on the quality of the force field parameters. Of course, the assumption that all relevant conformations have been located is major, and in many cases exhaustive conformational searches are not viable when one considers the computational expense involved. Finally, MINTA includes solvation effects via employment of a continuum model.

Here, computation of $\Delta\Delta G_{L-D}$ values using the MINTA approach, and their correspondence with ee's will be investigated for a series of receptors designed for the enantioselective separation of carboxylic acids. Results will be presented for a family of receptors based on the cholic acid backbone (**1**, Figure 1) which show different ee's for *N*-acyl-α-amino acids (**3**, Figure 1).[36] Success of the computations is measured by the degree with which the computed MINTA $\Delta\Delta G_{L-D}$ values can be related to the experimental enantioselectivities.

II. Methodology

II.1. Receptor−Ligand Sytems. Guanidinium receptors (**1**) form well-defined salt bridges between two of the three guanidinium protons (at receptor position 3) and the substrate (**2**) carboxylate oxygens via two parallel H-bonds (Figure 1). By varying the structure of the subunits A and B at positions 7 and 12, respectively, enhanced selectivities can be obtained.[36,37] Shown in Figure 2 are prototype models **4**−**8** for subunits A and B and for which receptor **1**/*N*-acyl-α-amino acid ee values exist. In receptor **1**, the terminal methyl group of **4**−**8** from

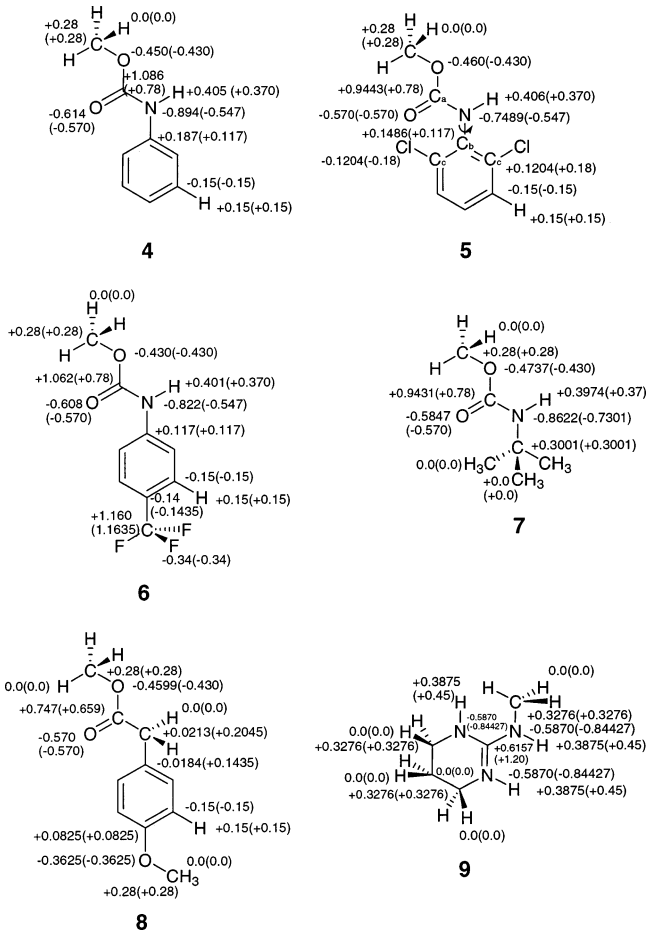

Figure 2. Models (**4**−**8**) of subunits A and B and guanidinium group (**9**) at position 3 for receptor **1** (Figure 1). The default MMFFs partial charges of all molecules **4**−**9** are reparametrized in this work. New partial charges are listed together with the default MMFFs values given in parentheses. For molecule **5,** new torsion parameters $H-N-C_b-C_c$ and $C_a-N-C_b-C_c$ were also derived for the rotation of the *o*-dichlorophenyl group as depicted above.

Figure 2 (top methyl group in each case) is replaced by a cholic acid six-membered ring $-CH_2-$ at either position 7 or 12. Our computations consist of studies for the binding of six receptors **1a**−**1f** (see results) with our chosen enantiomers, *N*-Ac-DL-valinate (**3** with R = isopropyl).

II.2. Free Energy Calculation Methodology. Computations of free energies using MINTA are preceded by separate extensive conformational searches to locate the lowest energy binding conformations of both enantiomers (L and D forms) to the chosen receptor. The highly efficient mixed mode MCMM/LMCS conformational search algorithm is used; a mixture of Monte Carlo multiple mimima (MCMM) steps,[38] where defined torsions are randomly adjusted, and low mode conformational search (LMCS) steps[39] which follows the low-frequency eigenvectors ("soft" vibrational modes) is used to direct the conformational search. The latter part uses the principles of saddle point location in an attempt to adequately cover the comformational space. This algorithm has been successfully applied to exhaustive conformational searches of organic compounds.[40] Our calculations are set up so that 50% of moves will be Monte Carlo torsional moves and/or global ligand translation and 50% low mode moves. For the torsional moves, 2 to $(N-1)$ torsions are varied per step where N is the number of defined torsions used in the search. Translation of the ligand in the binding pocket of the receptor is viewed as crucial to the success of the conformational search. Likewise, convergence of the number

of lowest energy conformers located or an exhaustive conformational search is critical for successful MINTA free energy calculations. Preliminary conformational searches indicated that 20 000 steps are required to reasonably sample the low-energy conformational space; the number of low-energy conformational states located after this point does not significantly increase. Hence, 20 000 MCMM/LMCS steps are chosen as a compromise between computational accuracy and efficiency. This corresponds to 950−1250 steps per torsional degree of freedom dependent on receptor subunits A and B. A MCSS (Monte Carlo structure selection) option is used as follows: the least investigated structure is used as the starting point for the next MC step (usage-directed structure selection) as opposed to the last-minimized structure (random-walk search). Energy windows are adjusted depending on receptor to reduce the number of low-energy conformers saved to a reasonable amount (generally, <1000).

Each conformation located from the MCMM/LMCS searches is reminimized in a "multiple minimization" procedure prior to the MINTA free energy calculations. This ideally eliminates duplicate conformations and improves the *conformations found: conformations with good convergence* ratios. For the MINTA calculations, conformers generated from the conformational search/multiple minimization schemes are used in separate free energy calculations ($T = 300$ K) of G_{R-L} and G_{R-D} for the receptor (R) bound L and D complexes, respectively.[41] The MINTA integrals are calculated as block averages with 10 × 1000 independent energy evaluations per conformation. Numerical integration in all degrees of freedom is used by default. In cases where this leads to numerical instabilities, only low-frequency "soft modes" are treated numerically with the less accurate but fast analytical MINTA integration used for the remainder degrees of freedom.[42] The default hard and soft limits for sampling along normal modes used are 1 Å and 3 units of standard deviation, respectively. Finally, the binding free energy difference is then calculated as the difference between the MINTA estimates for G_{R-L} and G_{R-D}:

$$\Delta\Delta G_{L-D} = G_{R-L} - G_{R-D} \tag{1}$$

All conformational searches, multiple minimizations, and MINTA computations are performed using either MacroModel 8.0 or 8.1.[43]

II.3. Force Field Employed. The original Merck (MMFFs) force field[44,45] or a reparametrized version (see below) is used, while solvation effects of chloroform are included using the GB/SA continuum model.[46−49] The original GB/SA model of Still et al.[46] has undergone huge improvements in recent times:[47−54] the present day accuracy combined with the computational efficiency of continuum solvation models such as GB/SA makes them highly competitive with explicit solvent models for many systems. In our study (see below), we find that the partial charges and torsion parameters are critical for accurate computation of binding preferences and thus the reproduction of experimental ee's. Partial charges are crucial as they largely serve to determine how successful the force field will be at describing solvation and the energetics of host−guest binding. Analysis of the MMFFs partial charges used in our calculations reveals that "fine-tuning" of partial charges is required to account for the different electronic effects in similar systems not accounted for by MMFFs. Torsion parameters are critical to obtaining the correct conformations. Insufficient torsion parameters are also highlighted and reparametrized. This paper is in essence a presentation of the results of these corrections and their effect on the accuracy of our BFE calculations using MINTA.

II.4. Partial Charge Extraction Procedure. The Merck force field uses a bond increment approach to calculation of partial charges, defined by eq 2.

$$q_i = q_i^0 + \sum W_{ji} \tag{2}$$

q_i^0 is an integral or fractional formal atomic charge, for example $+^1/_3$ for each guaninidium nitrogen and $-^1/_2$ for carboxylate oxygens (Figure 1). W_{ji} is the partial charge contribution to atom i from the $i-j$ bond with the sum over all atoms j to which i is bonded. The default MMFFs bond increments were obtained using a comprehensive iterative approach. Data from HF/6-31G* computations of dipole moments and electrostatic potential (ESP) fit charges at optimum geometries, and HF/6-31G* calculations of optimum hydrogen-bonded dimer geometries were all included in the fitting procedure. Note that although electron correlation effects are not accounted for, HF/6-31G* computations give a good account of hydrogen bonding.[44,55] Partial charges were obtained so as to obtain self-consistency between fits of the HF/6-31G* dipole moments, interaction energies, and hydrogen-bond geometries. For our reparametrization procedure, we use an approach similar in many ways to that used by the original Merck force field parametrization for fitting to the dipole moments.

A conformational search is first performed using the MCMM method for molecules **4**−**9** (exception molecule **5**), with the lowest energy conformer used as input for a subsequent HF calculation. In the case of molecule **5**, the lowest energy conformer is taken from computation of the MP2/6-31G* torsional profile (see below). Gas-phase HF/6-31G* optimizations of **4**−**9** follow, and the ESP of the optimum geometries is fitted to a set of partial charges.[56] The ESP fitting is further constrained to reproduce the dipole moments. A modified version of the program PAROPT for fitting to dipole moments is then used to extract the new force field partial charges (bond increments):[57,58] bond increments are adjusted in a least-squares RMSerr(μ) fit (eq 3) to the three HF/6-31G* calculated vector components, μ_x, μ_y, and μ_z, of the total dipole moment (μ_T) using the default MMFFs and new ESP fit charges as a guide.

$$\mathrm{RMSerr}(\mu) = \sqrt{\frac{1}{N}\sum_{i=x,y,z}(\mu_i^{FF} - \mu_i^{ai})^2} \tag{3}$$

μ_i^{FF} and μ_i^{ai} correspond to the force field and ab initio dipole moment components, respectively. An abstract temperature is used to control the Metropolis[59] simulating annealing schedule used in the parameter optimization schedule, and this temperature is manually adjusted at the start to yield an approximately 50% parameter acceptance ratio. This ratio is then approximately maintained during the parameter optimization procedure. As parameter fits to dipole moments are not unique, constraints are necessary and some are adopted from the original MMFFs parametrization: polar hydrogens are fixed at bond charge increments from the calculated HF/6-31G* ESP fit values, and original MMFFs bond increments for hydrogens attached to saturated aliphatic and aromatic carbons are retained. Further constraints are imposed by applying parameter maximum and minimum values to keep charges reasonably in agreement with the original MMFFs parameters: "fine-tuning" of parameters. The resulting parameters are a fit of bond charge increments

(partial charges) to reproduce μ_x, μ_y, and μ_z and which reflect, for the most part, trends observed in the HF/6-31G* charges.

All ab initio computations are performed using Jaguar,[60] and as stated, an extended version of PAROPT is used for all partial charge reparametrizations.

II.5. Torsion Parameter Extraction Procedure. Molecule **5** requires further reparametrization for the rotation of the *o*-dichlorophenyl group around the C−N bond shown in Figure 2. The rotational profile is generated at two ab initio levels, HF/6-31G* and MP2/6-31G*. Constraints are applied so that the rotation is symmetric with respect to the two H−N−C_b−C_c and two C_a−N−C_b−C_c torsion angles while every other internal coordinate is optimized. V_1, V_2, and V_3 parameters of the triple cosine torsional potential (eq 4) employed by the Merck force field are fitted to reproduce the torsional energy profile generated by the MP2/6-31G* calculations.

$$V = V_1/2(1 + \cos\theta) + V_2/2(1 - \cos 2\theta) + V_3/2(1 + \cos 3\theta) \quad (4)$$

The original PAROPT program[57] is used to obtain the best least-squares energy fit according to eq 5:

$$\mathrm{RMSerr}(V) = \sqrt{\frac{1}{N}\sum_{i=1}^{N}(V_i^{\mathrm{FF}} - V_i^{\mathrm{ai}})^2} \quad (5)$$

where V_i^{FF} and V_i^{ai} are the force field and ab initio energies, respectively, and N is the number points on the energy profile considered.

II.6. DFT Calculations. B3LYP/3-21+G* single point energy (SPE) calculations are performed to probe the quality of the different force fields with respect to their geometry predictions for the lowest energy L- and D-bound conformations. Chloroform solvation effects are included in these calculations using a self-consistent reaction field (SCRF) method.[61,62] The quantitative values of these energies will not be accurate at this level, but computational expense considerations prohibits our use of a basis set larger than 3-21+G* for these systems even for SPE calculations. All computations are performed using Jaguar.[60]

III. Results and Discussion

III.1. Accuracy of MMFFs Compared with Experiment for Prediction of Low-Energy Conformations. MMFFs[45] is an extension of the MMFF force field[44] that enforces planarity about delocalized sp^2 nitrogens and is therefore especially suitable for our carbamate functionalized receptors (Figure 2). The MMFFs force field shows good agreement with the previously obtained ^{1}H NMR and NOE data, and AMBER* molecular modeling results for binding preferences in these systems.[36,37] The MMFFs global minimum complexes located for receptor **1a** (subunits A = **5**, B = **4**) with *N*-Ac-DL-valinate are shown in Figure 3, where we can see the different binding associated with each enantiomer. Both complexes have parallel salt bridges between the carboxylate oxygens and guanidinium protons. The difference in binding arises from different interactions with subunits A and B. For the L-bound complex, the carboxylate also has a H-bond from the carbamate (position 7) NH, while the ligand acetyl oxygen accepts a H-bond from the carbamate (position 12) NH. This is consistent with the ^{1}H NMR data where the receptor carbamate N*H*'s (positions 7 and 12) and 2 of the 3 guanidinium N*H* signals move downfield on complex formation.[36,37] Also, a weak intermolecular NOE from the ligand α-C*H* to carbamate ortho protons at position 12 (although not clear from Figure 3(a)) is in support of our structure.[36,37] Extensive broadening in the experimental ^{1}H NMR spectra for the D-bound complex[36,37] prevents us from making an equally detailed analysis of our structure in Figure 3(b).

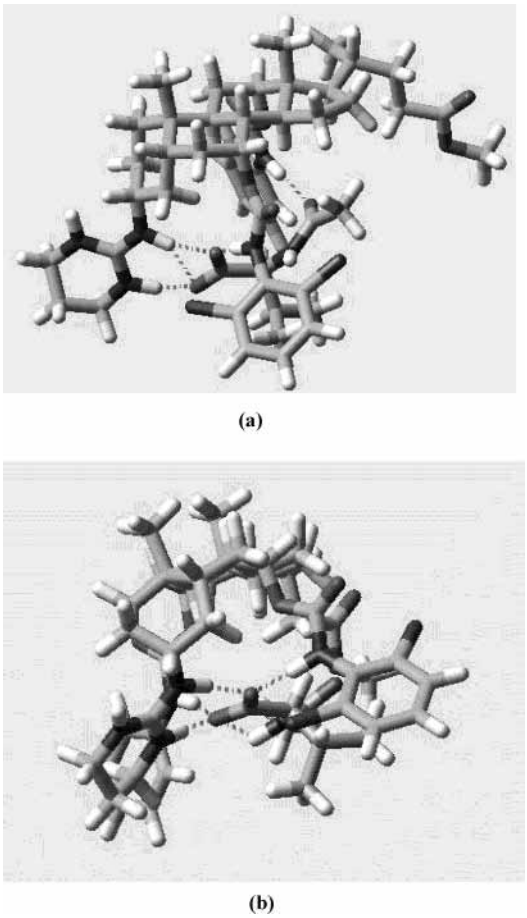

Figure 3. Using the MMFFs force field, lowest energy conformations located for binding of **(a)** L and **(b)** D forms of *N*-Ac-valinate to receptor **1** with subunits **5** and **4** for A and B, respectively (see Figures 1 and 2).

III.2. Comparison of Computed $\Delta\Delta G_{L-D}$ Values with Experimental ee's. Default MMFFs Force Field Results. Results of the conformational search/MINTA computations for receptors **1a**−**1f** with *N*-Ac-DL-valinate are presented in Table 1. **1a**−**1f** are as defined in Table 1 with different subunits **4**−**8** for A and B (Figure 2) as described in the Methodology section. Listed are the $\Delta\Delta H_{L-D}$ values which correspond to the difference in enthalpy between the lowest L- and D-bound conformations and the MINTA computed binding free energy differences at 300 K which can be compared with experiment;[63] the relative ordering (or rank) of the magnitude of $\Delta\Delta G_{L-D}$ values can be compared directly with the experimental ee's to analyze the efficiency of our computations.

We consider first the results for the default MMFFs parametrization. With respect to the relative ordering of computed $\Delta\Delta G_{L-D}$ values, we see that poor agreement with the experimental ee's is observed (Table 1): only the ordering of receptors **1e** and **1f** are correct. Receptor **1a** appears especially problematic where a rank of 4 compares with 1 for experiment; receptors **1b** and **1c** show equality with respect to selectivity ($\Delta\Delta G_{L-D}$ = −4.9 kcal mol^{-1}), while in practice **1b** (ee = 9:1) is more effective than **1c** (ee = 7:1) in chiral separation experiments. Finally, we note the effects of temperature and entropy are not uniform; $\Delta\Delta H_{L-D}$ and $\Delta\Delta G_{L-D}$ values differ to varying degrees

TABLE 1: Results of Successive Reparametrizations for Reproduction of Experimental Enantioselectivity (ee) Trends of Different Receptors for *N*-Ac-DL-valinate[a]

		side chain units[b]					
		A = **5** B = **4**	A = **6** B = **6**	A = **4** B = **4**	A = **7** B = **4**	A = **8** B = **4**	A = −OH B = **4**
	receptor	**1a**	**1b**	**1c**	**1d**	**1e**	**1f**
experiment[c]	ee	9:1	9:1	7:1	4:1	2:1	1:1
	$\Delta\Delta G_{L-D}$	−1.3	−1.3	−1.2	−0.8	−0.4	0.0
	relative ordering	*1*	*1*	*3*	*4*	*5*	*6*
MMFFs[d]	$\Delta\Delta H_{L-D}$	−3.4	−5.1	−5.1	−4.8	−1.1	−1.4
	$\Delta\Delta G_{L-D}$	−3.3	−4.9	−4.9	−3.9	−0.6	0.0
	relative ordering	*4*	*1*	*1*	*3*	*5*	*6*
reparametrization (step I)[e]	$\Delta\Delta H_{L-D}$	−3.1	−4.6	−4.3	−3.7	−2.2	0.1
	$\Delta\Delta G_{L-D}$	−2.8	−4.4	−4.4	−3.3	−1.2	0.5
	relative ordering	*4*	*1*	*1*	*3*	*5*	*6*
reparametrization (step II)[f]	$\Delta\Delta H_{L-D}$	−3.1	−4.4	−4.0	−3.5	−1.0	0.3
	$\Delta\Delta G_{L-D}$	−3.1	−3.9	−3.6	−3.2	−0.4	0.7
	relative ordering	*4*	*1*	*2*	*3*	*5*	*6*
reparametrization (step III)[g]	$\Delta\Delta H_{L-D}$	−4.3	−4.4	−4.0	−3.5	−1.0	0.3
[MMFFs*]	$\Delta\Delta G_{L-D}$	−3.8 [−3.84]	−3.9 [−3.88]	−3.6	−3.2	−0.4	0.7
	relative ordering	*1*	*1*	*3*	*4*	*5*	*6*

[a] Units for $\Delta\Delta H_{L-D}$ and $\Delta\Delta G_{L-D}$ (300 K) are kcal mol^{-1}. [b] Side chain units A and B (**4**−**8**, Figure 2) define receptor **1** (Figure 1). In receptor **1**, the terminal methyl groups of **4**−**8** (top methyl groups, Figure 2) are replaced by cholic acid six membered ring $-CH_2-$ groups at positions 7 and 12. [c] Reference;[36] experimental $\Delta\Delta G_{L-D}$ values are extracted from the relation: ln ee = $-\Delta\Delta G_{L-D}/RT$. [d] MMFFs: original MMFFs force field. [e] Reparametrization (step I) = MMFFs with reparametrized partial charges for subunits A and B. [f] Reparametrization (step II) = reparametrization (step I) + reparametrized partial charges for guanidinium group. [g] Reparametrization (step III) [MMFFs*] = reparametrization (step II) + reparametrized torsion parameters for rotation of the *o*-dichlorophenyl group around the C−N bond shown for **5** in Figure 2 (see text for details).

depending on receptor, from 0.1 kcal mol^{-1} for receptor **1a** to 1.4 kcal mol^{-1} for receptors **1f**. Inclusion of these effects is therefore crucial.

Close analysis of the computations performed reveals two problems. First, the partial charges on the carbamate subunits A and B (**4**−**7**) of the receptors. Specifically, the Merck force field uses the same "core" R−O−C(=O)−N(H)−R′ carbamate partial charges irrespective of the type of terminal R and R′ groups. Hence, for subunits A and B of receptors **1a**−**1f**, steric effects are accounted for but not the important electronic effects of (for example) having different substituents on the carbamate phenyl rings **4**, **5,** and **6**. These need reparametrization, and for consistency all subunits **4**−**9** in Figure 2 are reparametrized. Next, our results for receptor **1a** indicate parameter deficiencies with respect to the torsion parameters employed, in particular the rotation around the C−N bond in subunit A (**5**, Figure 2). Torsion parameters are crucial to obtaining the correct conformational preferences and energetics of molecular species.[28] Analysis of the Merck force field default dihedral potential parameters for torsion angles *i*−*j*−*k*−*l* reveals that the force field defines parameters solely based on the central *j*−*k* bond around which rotation occurs. Hence, the effect of different types of terminal atoms (*i* and *l*) attached to the central bond is not accounted for, and instead "wildcards" are used (**−*j*−*k*−**). For rotation of the *o*-dichlorophenyl group (**5**) around C−N the same parameters are used as those for an unsubstituted phenyl group (**4**). As expected, therefore, analysis of the MMFFs torsion profile for model compounds **4** and **5** reveals global minimum-energy structures with similar conformations. Clearly, this is incorrect, and adjustments are required.

Reparametrization Results (Step I). As a first step, all of the molecules **4**−**8** corresponding to models for subunits A and B are reparametrized for partial charges. Conformational searches followed by HF/6-31G* computations as described in the computational details were performed and charges (bond increments) then fitted to reproduce the ab initio dipole moments (eq 3). The results of these fits are presented in Table 2, and the new partial charges are listed with the old (default MMFFs) for each molecule in Figure 2. We see that all fits result in a huge improvement in the dipole moments despite the strict constraints imposed in the fitting procedure. The RMSerr(μ) using default MMFFs is large in all cases, most notably for molecule **6** (1.124 D). Following reparametrization, the RMSerr(μ) fits are a huge improvement from the original values computed using default MMFFs, most notably for molecules **4** and **7** where RMSerr(μ) fits of 0.0 D are obtained.

TABLE 2: Root-Mean-Square Fits (RMSerr(μ), Eq 3) of the Partial Charges (Bond Increments, Eq 2) of Model Compounds 4−9 (Figure 2) To Reproduce the HF/6-31G* Dipole Moment Components (Debye)

molecule	method	μ_x	μ_y	μ_z	μ	RMSerr(μ)
4	MMFFs	−2.350	1.762	0.0	2.937	0.592
	HF/6-31G*	−2.225	0.744	0.0	2.346	0.0
	fit	−2.218	0.746	0.0	2.340	0.004
5	MMFFs	−1.123	2.247	1.182	2.776	0.514
	HF/6-31G*	−0.845	1.648	0.584	1.942	0.0
	fit	−1.044	1.620	0.562	2.008	0.117
6	MMFFs	2.573	0.763	−2.940	3.981	1.124
	HF/6-31G*	3.629	2.278	−2.323	4.874	0.0
	fit	3.280	1.884	−2.342	4.449	0.304
7	MMFFs	−2.293	1.424	0.0	2.699	0.276
	HF/6-31G*	−2.089	0.992	0.0	2.313	0.0
	fit	−2.089	0.992	0.0	2.313	0.0
8	MMFFs	−0.979	2.478	−0.201	2.672	0.588
	HF/6-31G*	−0.553	1.662	0.233	1.767	0.0
	fit	−0.636	1.757	0.402	1.911	0.122
9	MMFFs	−2.726	−0.640	0.651	2.875	0.711
	HF/6-31G*	−1.560	−0.285	0.471	1.654	0.0
	fit	−2.209	−0.595	0.651	2.379	0.428

The Merck force field with new partial charges for subunits A and B was then tested in further conformational search/

TABLE 3: Results of Rotational Profile in kcal mol^{-1} for Rotation of an *o*-Dichlorophenyl Group around the C−N Bond Shown for 5 in Figure 2[a]

	angle (deg)					
method[b]	0	25	45	65	75	90
HF/6-31G*	14.83	7.26	2.48	0.29	0.03	0.00
MP2/6-31G*	14.09	7.47	2.97	0.23	0.00	0.13
MMFFs	3.91	0.00	1.15	4.75	6.42	7.52
reparametrization (step II)/tors = 0	20.40	12.27	5.65	1.49	0.49	0.00
reparametrization (step III) [MMFFs*]	13.97	7.00	2.45	0.36	0.06	0.00

[a] Due to the symmetry constraints imposed, the profile repeats itself every 90°. [b] MMFFs: profile using default MMFFs parameters; reparametrization (step II)/tors = 0: force field profile with the new partial charges, but the torsion parameters for the $C_a-N-C_b-C_c$ and $H-N-C_b-C_c$ angles set to zero; reparametrization (step III) [MMFFs*]: profile with new partial charges and refined torsional parameters (listed in Table 4) for the $C_a-N-C_b-C_c$ and $H-N-C_b-C_c$ angles of **5** which were fitted to the MP2/6-31G* energies.

MINTA computations for any improvement in the BFE results. From Table 1 (reparametrization (step I)), we see that although the magnitude of the $\Delta\Delta G_{L-D}$ (and $\Delta\Delta H_{L-D}$) values has changed, the ordering of the receptors with respect to experiment is still the same. As a next step, we additionally reparametrize the partial charges of the guanidinium group **9** at position 3 (**1**, Figure 1).

Reparametrization Results (Step II). On comparing the HF/6-31G* guanidinium (**9**) ESP fit charges with the default MMFFs values, we note that the differences are quite large: the HF/6-31G* proton charges are +0.3875 (average), while the MMFFs default values are substantially more positive (+0.450); also, the ESP partial charge for C connected to all three N's is +0.7391 compared with +1.200 for MMFFs. The MMFFs +0.45 partial charge is in fact a Mulliken-based partial charge. Although this charge and guanidinium partial charges were fitted to reproduce interaction energies and hydrogen-bonding geometries, we view uniform parametrization against HF/6-31G* data for subunits at all three positions 3, 7, and 12 of receptor **1** (Figure 1) to be crucial to ensure a proper balance of interactions between receptor, substrate, and solvent. Indeed, balance is seen as an essential element if reliable results are to be obtained in condensed phase simulations.[65] The guanidinium group is hence reparametrized to reflect better the HF/6-31G* trends. A further constraint was imposed in the optimization procedure with guanidinium protons fixed at the average of their HF ESP fit values (+0.3875). The results of the fit of partial charges (bond increments) to dipole moments for **9** are also presented in Table 2. Reparametrization improves the RMSerr-(μ) for dipole moment components from 0.711 to 0.428 D. The new parameters were then tested in further conformational search/MINTA computations in combination with the already reparametrized charges for subunits A and B from reparametrization (step I). From Table 1, we now see a dramatic improvement in the ordering of $\Delta\Delta G_{L-D}$ values relative to experiment. Receptor **1a** is now the only receptor that does not follow the experimental (ee) sequence. Its value for $\Delta\Delta G_{L-D}$ of −3.1 kcal mol^{-1} compares with a value of −3.9 kcal mol^{-1} for receptor **1b** which experimentally shows the same enantioselectivity (ee = 9:1). As a next step, the deficient torsion parameters of subunit A of receptor **1a** are reparametrized.

Reparametrization Results (Step III)/ MMFFs*. The results of the reparametrization of the $H-N-C_b-C_c$ and $C_a-N-C_b-C_c$ torsion angles for **5** (Figure 2) are presented in Tables 3 and 4. Shown in Table 3 are the results for the rotational profile calculated at the HF/6-31G* and MP2/6-31G* levels. Also listed is the same profile for the default MMFFs torsion parameters; the energy profile with the reparametrized partial charges but torsion force constants for $H-N-C_b-C_c$ and $C_a-N-C_b-C_c$ angles set to 0 (reparametrization (step II)/tors = 0) and finally the new profile, again with the new partial charges but following reparametrization of these two torsion types (reparametrization (step III)/MMFFs*). Reparametrization was performed using the original PAROPT program so as to shift the values for "reparametrization (step II)/tors = 0" to be more in agreement with the MP2/6-31G* results. As the multiplicity of the potential is two (number of minimum points as C−N bond (Figure 2) is rotated through 360°) determined by our quantum mechanics calculations, eq 4 was truncated at second order with just V_1 and V_2 terms fitted to the MP2/6-31G* data. A best RMSerr(V) fit of 0.27 kcal mol^{-1} was obtained (eq 5). The new refined torsion parameters are listed in Table 4 and their profiles shown in Figure 4. The new parameters offer the best fit obtained with PAROPT and, most importantly, reproduce the quantum mechanics conformational preferences. For the default MMFFs force field, the *o*-dichlorophenyl group is almost planar with the −C(=O)−N(H)− amide group. After reparametrization, the dichorophenyl is closer to being perpendicular in line with the MP2/6-31G* results. Further, the barrier height to rotation is well reproduced with the reparametrized model (14.15 kcal mol^{-1}), showing excellent agreement with 14.01 kcal mol^{-1} calculated at the MP2/6-31G* level (Table 4).

TABLE 4: Default MMFFs and New MMFFs* (Reparametrization (Step III)) Torsion Parameters with Corresponding Barrier Heights (Compared with MP2/6-31G* Value) for the Rotation around the C−N Bond of 5 Shown in Figure 2[a]

	torsion parameters						
	$C_a-N-C_b-C_c$			$H-N-C_b-C_c$			
method	V_1	V_2	V_3	V_1	V_2	V_3	barrier height
MMFFs	0.0	6.0	0.0	0.0	6.0	0.0	4.42
MMFFs*	0.0	0.7355	0.0	0.0	2.4795	0.0	14.15
MP2/6-31G*							14.01

[a] Parameters based on the standard triple cosine potential, eq 4; V_1-V_3 and "barrier height" (defined as energy for rotation of *o*-dichlorophenyl group from unconstrained global minimum through 0°) are given in kcal mol^{-1}.

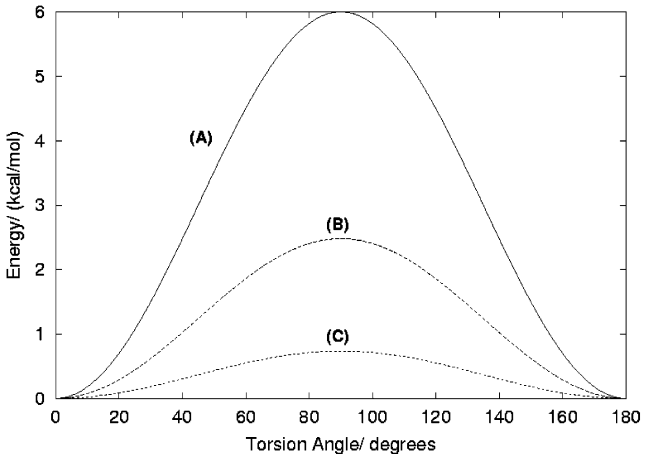

Figure 4. Torsion potentials used for rotation of **5** around the C−N bond shown in Figure 2. (A) is the default MMFFs *−C−N−* rotational profile. $C_a-N-C_b-C_c$ and $H-N-C_b-C_c$ torsion angles have the same parameters and hence the same rotational profile. (B) and (C) are the reparametrized $C_a-N-C_b-C_c$ and $H-N-C_b-C_c$ rotational profiles, respectively. The new force field parameters are given in Table 4.

TABLE 5: DFT(B3LYP/3-21+G*) Absolute and Relative Energies for the Global Minima L- and D-Bound Complexes of *N*-Ac-valinate to Receptor 1a Obtained Using MMFFs Default and Reparametrized Force Fields[a]

		energies	
complex	force field	absolute (a.u.)	relative (kcal mol^{-1})
L	MMFFs	−3853.600 64	0.0
	reparametrized MMFFs (step I)	−3853.593 32	+4.6
	reparametrized MMFFs (step II)	−3853.593 82	+4.3
	reparametrized MMFFs (step III)/[MMFFs*]	−3853.610 83	−6.4
D	MMFFs	−3853.585 80	0.0
	reparametrized MMFFs (step I)	−3853.578 00	+4.9
	reparametrized MMFFs (step II)	−3853.580 83	+3.1
	reparametrized MMFFs (step III)/[MMFFs*]	−3853.603 63	−11.2

[a] Receptor **1a** = receptor **1** (Figure 1) with subunits for A and B of **5** and **4**, respectively (Figure 2). Energies are based on single point energy (SPE) calculations at the global minima geometries obtained from MCMM/LMCS conformational searches. $CHCl_3$ solvation effects are included in all calculations using a self-consistent reaction field (SCRF) model.[61,62] (The MMFFs global minimum geometries are shown in Figure 3).

Combining the new torsion parameters with the complete set of reparametrized charges from steps I and II, we arrive at our final set of parameters, MMFFs* (a partially adjusted MMFFs parameter set). MMFFs* is then applied to recomputation of $\Delta\Delta G_{L-D}$ for receptor **1a**; MMFFs* values of $\Delta\Delta G_{L-D}$ for receptors **1b**−**1f** will be as for step II. From Table 1, MMFFs* (reparametrization (step III)), we see that the calculated results for $\Delta\Delta G_{L-D}$ are now in nearly complete agreement with the qualitative trends for ee's ($\Delta\Delta G_{L-D}$ for **1a** [−3.84] ≈ $\Delta\Delta G_{L-D}$ for **1b** [−3.88]). Hence, we now almost reproduce the correct relative ordering for receptor enantioselectivity of **1a** ≈ **1b** > **1c** > **1d** > **1e** > **1f**. Our new parameter set MMFFs* hence offers a large improvement over the results obtained using the original Merck force field. While large discrepancies in Table 1 exist for default MMFFs, the qualitative experimental trends in enantioselectivity for the chiral selective receptors are close to completely reproduced using MMFFs* in MINTA computations of $\Delta\Delta G_{L-D}$.

III.3. Performance of New Parameters in Terms of Structural Features. While the original MMFFs partial charges extraction procedure includes a combination of fits to dipole moments, interaction energies, and hydrogen-bond geometries, the partial charges we obtain are fitted only to dipole moments. For this reason, we adopted constraints used in the original parametrization, and parameters were held reasonably close to their original MMFFs values using the HF/6-31G* ESP fit charges as a guide. These parameters, in combination with refined torsions, are able to describe qualitative $\Delta\Delta G_{L-D}$ trends compared with experimental enantioselectivities, but how do they compare with respect to *geometries* of the "global" optimum conformations located?

Table 5 contains a comparison of DFT (B3LYP/3-21+G*) SPEs for the global minimum conformations of the receptor **1a**/*N*-Ac-DL-valinate system obtained using the default MMFFs force field; MMFFs force field including reparametrizations from steps I and II; and our final MMFFs* parameter set (reparametrization step III) which includes all reparametrizations. The fully reparametrized MMFFs* parameter set (partial charges and torsions) geometry predictions for global minima are by far the lowest in energy; MMFFs* L- and D- bound complexes are 6.4 and 11.2 kcal mol^{-1} lower in energy, respectively, than those of default MMFFs at this level of theory. The geometries with all partial charges reparametrized, reparametrization (step II) (guanidinium group; subunits A and B), give a better balance with respect to binding than those obtained with just new partial charges for subunits A and B (reparametrization (step I)), and this is reflected in slightly lower B3LYP/3-21+G* energy values. The sharp drop in complex energies from reparametrization step II to final MMFFs* (about 10−15 kcal mol^{-1}), where torsion parameters are also corrected, is indicative of the importance of torsion potentials to correct conformational predictions. Meanwhile, the geometries for default MMFFs are slightly better than those of reparametrizations steps I and II with only partial charges reparametrized. Although this may originate from a fortuitous cancellation of errors, this is also not totally unexpected as the partial charges for MMFFs were obtained using a comprehensive iterative procedure which included fits to reproduce hydrogen-bonding distances. The reparametrized partial charges obtained here are crude, fitted solely to dipole moment components, but fulfill their objective to reflect the trends in binding preferences ($\Delta\Delta G_{L-D}$ differences) between similar receptors on the basis of HF/6-31G* computations. A more elaborate approach might in the future fit to a combination of dipoles and hydrogen-bonding distances inclusive. This, however, was beyond the intended scope of the project here.

IV. Summary and Conclusions

The effectiveness of MINTA as applied to calculation of BFE differences ($\Delta\Delta G_{L-D}$) for chiral selective receptors has been shown. Note that numerical errors in MINTA calculations due to neglect of rotational and translational contributions to the configuration integral[66] were not a problem for the systems here, just as in other published applications of MINTA.[34,35] Only relative free energies for binding of L and D enantiomers to similar type receptors were calculated, and hence the conformational changes studied do not significantly alter the rotational moments of inertia. Hence, the rigid-rotor approximation employed by MINTA is still valid for our systems. While deficiencies in the original MMFFs force field lead to large discrepancies between computation and experiment, on systematic reparametrization of crucial partial charges and torsions directly involved in the binding of substrate, computed MINTA $\Delta\Delta G_{L-D}$ values for a series of receptors obtained can be qualitatively related to the available experimental enantioselectivities. The new torsion parameters were extracted using the program PAROPT, while a modified version of PAROPT was used to fit partial charges to dipole moments under strict physical constraints. The dependence of MINTA accuracy on the quality of force field parameters employed has hence been highlighted, but also the applicability of the novel MINTA approach to calculation of binding affinities. A new fundamental method for calculation of binding affinities using refined critical force field parameters and MINTA has been proposed. We are now using this method to propose potential new and better synthetic receptors for *N*-acyl-α-amino acids on the basis on computation alone.

The use of MINTA with refined force field parameters method was successfully applied here to a chiral recognition study with medium-sized receptors. However, this may form the basis for application of the approach to a much broader range of receptor−ligand type system: molecular recognition studies and the binding of ligands in protein pockets are a few examples. Since MINTA's focus on low-energy conformations proved not to be a problem for our medium-sized receptor−enantiomer type complexes, the on average higher barriers for movements of a ligand in a protein−ligand complex suggest the same. Moreover, with respect to implicit solvation models, a new continuum treatment for long-range interactions has also been successfully applied to protein−ligand binding.[67] Of course, MINTA success is dependent on the location of all relevant (low-energy) minima in the conformational space—a problem which is significantly magnified for protein−ligand systems compared to our medium-sized sytems studied here. Also, reparametrization of force field parameters for a given protein is an enormous amount of work and is generally not feasible. However, reparametrizations of ligands, and/or the crucial atom types in the active site of a protein, may provide the key to success.

Acknowledgment. We are grateful to István Kolossváry for assistance with the MINTA computations and also to Schrödinger Inc., particularly John Shelley and Gerd Räther for MacroModel and Jaguar technical support, respectively. Financial support for this project comes in part from the European Union (HPRN-CT-2001-00182): "Enantioselective Recognition: Towards the Separation of Racemates".

References and Notes

(1) Rouhi, A. M. *Chem. Eng. News* **2002**, *80* (23), 43−50.
(2) DesJarlais, R. L.; Sheridan, R. P.; Seibel, G. L.; Dixon, J. S.; Kuntz, I. D.; Venkataraghavan, R. *J. Med. Chem.* **1988**, *31*, 722−729.
(3) Verkhivker, G.; Appelt, K.; Freer, S. T.; Villafranca, J. E. *Protein Eng.* **1995**, *8*, 677−691.
(4) Böhm, H. J. *J. Comput.-Aided Mol. Design* **1994**, *8*, 243.
(5) McMartin, C.; Bohacek, R. S. *J. Comput.-Aided Mol. Des.* **1997**, *11*, 333−344.
(6) Glide 2.7, Schrödinger, L. L. C.; New York, 1991−2003.
(7) Tomioka, N.; Itai, A.; Iitaka, Y. J. *J. Comput.-Aided Mol. Des.* **1987**, *1*, 197−210.
(8) Zwanzig, R. W. *J. Chem. Phys.* **1954**, *22*, 1420−1426.
(9) Mezei, M.; Beveridge, D. L. *Ann. N.Y. Acad. Sci.* **1986**, *482*, 1−23.
(10) Mruzik, M. R.; Abraham, F. F.; Schreiber, D. E.; Pound, G. M. *J. Chem. Phys.* **1976**, *64*, 481−491.
(11) Mezei, N.; Swaminathan, S.; Beveridge, D. L. *J. Am. Chem. Soc.* **1978**, *100*, 3255−3256.
(12) Kollman, P. *Chem. Rev.* **1993**, *93*, 2395−2417.
(13) Murcko, A.; Murcko, M. A. *J. Med. Chem.* **1995**, *38*, 4953−4967.
(14) Warshel, A.; Russell, S. T. *Q. Rev. Biophys.* **1984**, *17*, 283−422.
(15) Orozco, M.; Luque, F. J. *Chem. Phys. Lett.* **1997**, *265*, 473−480.
(16) Aqvist, J.; Medina, C.; Samuelsson, J. E. *Protein Eng.* **1994**, *7*, 385−391.
(17) Pierce, A. C.; Jorgensen, W. L. *J. Med. Chem.* **2001**, *44*, 1043−1050.
(18) Rizzo, R. C.; Tirado-Rives, J.; Jorgensen, W. L. *J. Med. Chem.* **2001**, *44*, 145−154.
(19) van Gunsteren, W. F.; Mark, A. E. *Eur. J. Biochem.* **1992**, *204*, 947−961.
(20) Mitchell, M. J.; McCammon, J. A. *J. Comput. Chem.* **1991**, *12*, 271−275.
(21) Mark, A. E.; van Helden, S. P.; Smith, P. E.; Janssen, L. H. M.; van Gunsteren, W. F. *J. Am. Chem. Soc.* **1994**, *116*, 6293−6302.
(22) Kollman, P. A. *Acc. Chem. Res.* **1996**, *29*, 461−469.
(23) McDonald, D. Q.; Still, W. C. *Tetrahedron Lett.* **1992**, *33*, 7747−7750.
(24) Lamb, M. L.; Jorgensen, W. L. *Curr. Opin. Chem. Biol.* **1997**, *1*, 449−457.
(25) Gilson, M. K.; Given, J. A.; Bush, B. L.; McCammon, J. A. *Biophys. J.* **1997**, *72*, 1047−1069.
(26) Essex, J. W.; Severance, D. L.; Jorgensen, W. L. *J. Phys. Chem. B* **1997**, *101*, 9663−9669.
(27) Guarnieri, F.; Still, W. C. *J. Comput. Chem.* **1994**, *15*, 1302−1310.
(28) McDonald, D. Q.; Still, W. C. *J. Am. Chem. Soc.* **1994**, *116*, 11550−11553.
(29) Senderowitz, H.; Guarnieri, F.; Still, W. C. *J. Am. Chem. Soc.* **1995**, *117*, 8211−8219.
(30) Senderowitz, H.; McDonald, D. Q.; Still, W. C. *J. Org. Chem.* **1997**, *62*, 9123−9127.
(31) Wang, J.; Dixon, R.; Kollman, P. A. *Proteins* **1999**, *34*, 69−81.
(32) Wall, I. D.; Leach, A. R.; Salt, D. W.; Ford, M. G.; Essex, J. W. *J. Med. Chem.* **1999**, *42*, 5142−5152.
(33) Head, M. S.; Given, J. A.; Gilson, M. K. *J. Phys. Chem. A* **1997**, *101*, 1609−1618.
(34) Kolossváry, I. *J. Phys. Chem. A* **1997**, *101*, 9900−9905. Kolossváry, I.; US Patent Serial No. 08/940, 145, Mode Integration (MINTA): Method and Apparatus for Selecting a Molecule Based on Conformational Free Energy.
(35) Kolossváry, I. *J. Am. Chem. Soc.* **1997**, *119*, 10233−10234.
(36) Lawless, L. J.; Blackburn, A. G.; Ayling, A. J.; Pérez-Payán, M. N.; Davis, A. P. *J. Chem. Soc., Perkin Trans. 1* **2001**, 1329−1341.
(37) Davis, A. P.; Lawless, L. J. *Chem. Commun.* **1999**, 9−10.
(38) (a) Chang, G.; Guida, W. C.; Still, W. C. *J. Am. Chem. Soc.* **1989**, *111*, 4379−4386. (b) Chang, G.; Guida, W. C.; Still, W. C. *J. Am. Chem. Soc.* **1990**, *112*, 1419−1427.
(39) Kolossváry, I.; Guida, W. C. *J. Am. Chem. Soc.* **1996**, *118*, 5011−5019.
(40) Greenidge, P. A.; Merette, S. A.; Beck, R.; Dodson, G.; Goodwin, C. A.; Scully, M. F.; Spencer, J.; Weiser, J.; Deadman, J. J. *J. Med. Chem.* **2003**, *46*, 1293−1305.
(41) The BFE for binding of the L enantiomer to a receptor R can be calculated: $\Delta G_L = G_{R-L} - G_R - G_L$. An analogous equation exists for binding of the D enantiomer. As the isolated enantiomeric free energies are the same ($G_L = G_D$), the BFE difference $\Delta\Delta G_{L-D}$, can be calculated from knowledge of just G_{R-L} and G_{R-D}: $\Delta\Delta G_{L-D} = G_{R-L} - G_{R-D}$.
(42) Note that two sample MINTA calculations were performed on one of our receptor−ligand systems to compare the effect of numerically integration over the first 20 versus the first 100 lowest energy modes. The effect on the values of $\Delta\Delta G_{L-D}$ was found to be minimal.
(43) Mohamadi, F.; Richards, N. G. J.; Guida, W. C.; Liskamp, R.; Lipton, M.; Caufield, C.; Chang, G.; Hendrickson, T.; Still, W. C. *J. Comput. Chem.* **1990**, *11*, 440−467. MacroModel 8.0 and 8.1, Schrödinger, L. L. C., New York, 1991−2003.
(44) Halgren, T. A. *J. Comput. Chem.* **1996**, *17*, 490−512, 520−552, 553−586, 587−615, 616−641.
(45) Halgren, T. A. *J. Comput. Chem.* **1999**, *20*, 720−729, 730−748.
(46) Still, W. C.; Tempczyk, A.; Hawley, R. C.; Hendrickson, T. *J. Am. Chem. Soc.* **1990**, *112*, 6127−6129.
(47) Weiser, J.; Shenkin, P. S.; Still, W. C. *J. Comput. Chem.* **1999**, *20*, 217−230.
(48) Weiser, J.; Weiser, A. A.; Shenkin, P. S.; Still, W. C. *J. Comput. Chem.* **1998**, *19*, 797−808.
(49) Weiser, J.; Shenkin, P. S.; Still, W. C. *J. Comput. Chem.* **1999**, *20*, 586−596.
(50) Ghosh, A.; Rapp, C. S.; Friesner, R. A. *J. Phys. Chem. B* **1998**, *102*, 10983−10990.
(51) Cramer, C. J.; Truhlar, D. G. *Chem. Rev.* **1999**, *99*, 2161−2200.
(52) Orozco, M.; Luque, F. J. *Chem. Rev.* **2000**, *100*, 4187−4225.
(53) Guvench, O.; Weiser, J.; Shenkin, P. S.; Kolossváry, I.; Still, W. C. *J. Comput. Chem.* **2002**, *23*, 1−8.
(54) Gallicchio, E.; Zhang, L. Y.; Levy, R. M. *J. Comput. Chem.* **2002**, *23*, 517−529.
(55) Pranata, J.; Wierschke, S. G.; Jorgensen, W. L. *J. Am. Chem. Soc.* **1991**, *113*, 2810−2819.
(56) (a) Chirlian, L. E.; Francl, M. M. *J. Comput. Chem.* **1987**, *8*, 894−905. (b) Woods, R. J.; Khalil, M.; Pell, W.; Moffat, S. H.; Smith, Jr., V. H. *J. Comput. Chem.* **1990**, *11*, 297. (c) Breneman, C. M.; Wiberg, K. B. *J. Comput. Chem.* **1990**, *11*, 361−373.
(57) Hayes, J. M.; Greer, J. C. *Comput. Phys. Commun.* **2002**, *147*, 803−825.
(58) The original PAROPT program was written to extract force field parameters by fitting to accurately calculated (quantum chemical) energies, forces, or a combination of a energies + forces. The modified version here extracts partial charge parameters by fitting to dipole moment components.
(59) Metropolis, N.; Rosenbluth, A.; Teller, A.; Teller, E. *J. Chem. Phys.* **1953**, *21*, 1087−1092.
(60) Jaguar 5.0, Schrödinger, L. L. C., New York, 1991−2003.
(61) Tannor, D. J.; Marten, B.; Murphy, R. A.; Friesner, R. A.; Sitkoff, D.; Nicholls, A.; Ringnalda, M.; Goddard, W. A., III.; Honig, B. *J. Am. Chem. Soc.* **1994**, *116*, 11875−11882.
(62) Marten, B.; Kim, K.; Cortis, C.; Friesner, R. A.; Murphy, R. B.; Ringnalda, M. N.; Sitkoff, D.; Honig, B. *J. Phys. Chem.* **1996**, *100*, 11775−11788.

(63) The individual G_{R-L} and G_{R-D} errors were found to range from $\sim\pm0.07$ to 0.2 kcal mol^{-1}; hence, errors for $\Delta\Delta G_{L-D}$ range from $\sim\pm0.15$ to 0.4 kcal mol^{-1}. These errors are still lower than one recent estimate (0.5 kcal mol^{-1}) of the highest level of accuracy for relative binding free energies today.[64]

(64) MacroModel 8.1 Reference Manual, Schrödinger, L. L. C., New York, 2003; p 236.

(65) MacKerrell, A. D., Jr.; Wiórkiewicz-Kuczera, J.; Karplus, M. *J. Am. Chem. Soc.* **1995**, *117*, 11946−11975.

(66) (a) Potter, M. J.; Gilson, M. K. *J. Phys. Chem. A* **2002**, *106*, 563−566. (b) Chang, C.-E.; Potter, M. J.; Gilson, M. K. *J. Phys. Chem. B* **2003**, *107*, 1048−1055.

(67) Simonson, T.; Archontis, G.; Karplus, M. *J. Phys. Chem. B* **1997**, *101*, 8349−8362.